5-12-2015

On the Fe Enrichment during Anodic Polarization of Mg and Its Impact on Hydrogen Evolution

D. Lysne
Boise State University

S. Thomas
Monash University

M. F. Hurley
Boise State University

N. Birbilis
Monash University

On the Fe Enrichment during Anodic Polarization of Mg and Its Impact on Hydrogen Evolution

D. Lysne,[a,b] S. Thomas,[b,*,z] M. F. Hurley,[a,*] and N. Birbilis[b,*]

[a]*College of Engineering, Department of Materials Science and Engineering, Boise State University, Boise, Idaho 83725, USA*
[b]*Department of Materials Engineering, Monash University, Clayton, Victoria 3800, Australia*

Iron (Fe) is an unintentional impurity present in pure magnesium (Mg) and Mg alloys, albeit nominally in low and innocuous concentrations (< 100 ppmw). Since Fe, like most metals, is more noble than Mg, the presence of Fe impurities can serve as cathodic sites within the Mg matrix. During anodic polarization of Mg, incongruent dissolution can lead to undissolved Fe impurities accumulating upon the Mg surface, permitting an increase in the overall rate of hydrogen evolution. The experimental manifestation of the incongruent dissolution of Mg, has not yet been clarified, wherein, the extent and efficiency of Fe enrichment during anodic polarization is not known, and also the increase in the hydrogen evolution rate due to Fe enrichment has not been quantified. In this work, Mg specimens with Fe concentration between 40 to 13,000 ppmw were examined in 0.1 M NaCl to obtain a quantitative relation between the Fe concentration and the rate of cathodic hydrogen evolution. These base-line alloys were then anodically polarized to facilitate surface Fe enrichment, and subsequently again cathodically polarized to determine the impact of prior dissolution and Fe enrichment on the subsequent hydrogen evolution. A simple model to predict Fe enrichment was used to analyze the electrochemical data and predict the extent and efficiency of Fe enrichment.

Manuscript submitted April 9, 2015; revised manuscript received April 30, 2015. Published May 12, 2015.

Iron (Fe) is one of the most common impurity elements present in commercially pure magnesium (Mg) and Mg-alloys.[1–4] Fe has a low solubility in Mg (∼0.018 wt%, or 180 ppmw)[1] and may be introduced via steel containers and melting/casting pots in Mg production.[1–3] Although the Fe pickup is relatively minor, the insolubility of Fe renders the impurity Fe to be dispersed as an insoluble body centred cubic (bcc) phase in the Mg matrix.[1] The corrosion of pure Mg, and Mg alloys can be strongly influenced by the presence of such Fe impurities.[1–9] Hanawalt and co-workers observed that an increase in the Fe (or impurity) concentration enhanced the corrosion rate of Mg and Mg alloys,[8–9] and proposed a "tolerance limit" for impurities; an empirically defined impurity concentration above which the corrosion rate of Mg increases drastically.[8–9] There exist tolerance limits for several insoluble metals in Mg, including Ni, Cu, Cr, Co, etc.[10] However, the focus of the work herein is the common impurity, Fe. For pure Mg, the tolerance limits for Fe was observed to be 170 ppm.[8]

Impurity Fe particles are nominally very fine (sub-micron) and difficult to image in pure Mg or Mg-alloys[11] and are usually detected from bulk inductively coupled plasma (ICP) analysis.[12–13] The Fe particles serve as micro/nano cathodes in the Mg matrix, and since Fe is much more noble than Mg, the driving force for micro-galvanic coupling between Fe and the Mg matrix is high (∼1 V) resulting in enhanced dissolution of the Mg matrix.

The hydrogen evolution reaction (HER) is the main cathodic reaction for Mg systems, whilst the HER has a high overpotential close to the typical open circuit potential of Mg and its alloys (which has OCPs in the range −1.5 to −1.8 V_{SCE}).[14–15] Any Fe particles or Fe containing particles in the Mg matrix thus experience significant cathodic polarization (at the Mg alloy OCPs), and the HER takes place at extremely high rates at such sites. It is now widely known that the HER on pure Mg increases during anodic polarization,[11,16–25] posing an anomaly on the conventional analysis of the mixed potential theory. A number of possible explanations for this phenomenon have been presented independently by several researchers,[25] however a holistic mechanistic explanation for enhanced HER upon Mg during anodic polarization still eludes the research community. One possible explanation is that during anodic polarization of pure Mg, the Fe impurities that do not dissolve into their aqueous ions (unlike Mg going to Mg^{2+}) may enrich or agglomerate upon the Mg surface. The rationale is that since Fe particles are cathodically polarized at all times (even during excessive anodic polarization of the bulk Mg), Fe is not oxidized, thus continually supporting reduction reactions. An increase in the Fe concentration upon the Mg surface will increase the net surface area of the cathode, resulting in an observed increase in HER. The measurement of the Fe concentration/enrichment on the anodically polarized Mg surface using analytical techniques is difficult, as the metal is covered by a dense oxide/hydroxide layer.[11] Therefore the extent and efficiency of the Fe enrichment effect during anodic polarization have not been clearly realized. The increase in the HER due to possible Fe enrichment has also not been quantified in the past.

The current work aims to explore the effect of Fe enrichment during anodic polarization on the electrochemical kinetics of the HER using two approaches. The first is via the use of custom prepared Mg ingots with different concentrations of Fe below and above the solubility limit (ranging from 40 to 13000 ppmw, as a result of deliberate Fe additions) which are anodically polarized, and then compared for their cathodic currents with their unpolarized counterparts. This helps one to deduce the impact of Fe enrichment on the rate of HER upon Mg. The second approach is one that can link the theoretical enrichment one may expect from low initial Fe content Mg specimens, with the response of higher Fe containing specimens. This will indicate, electrochemically, the efficiency of supposed Fe enrichment. To this end, a simple model for Fe enrichment during anodic polarization of the Mg has been used to analyze the electrochemical data, providing an initial quantification of the influence of Fe in regards to the HER.

Materials and Methods

Commercially pure Mg (with 40 ppm Fe), and Mg with Fe concentrations between 220 and 13,000 ppm (manufacture and characterization procedures described in[4,12–13]) were first successively ground to 2000 grit SiC paper, and then subjected to cathodic polarization in 0.1 M NaCl solution from OCP to −2.1 V_{SCE} using a scan rate of 1 mV/sec. This set of tests enabled collection of the base-line electrochemical data for analysis. The Mg samples with 40 ppm Fe and 220 ppm Fe were galvanostatically anodically polarized in 0.1 M NaCl, for different time periods (in seconds) and current densities (A/cm^2), to facilitate Fe enrichment. After this "pre-treatment", these samples were once again cathodically polarized to compare their behavior with

*Electrochemical Society Active Member.
[z]E-mail: Sebastian.Thomas@monash.edu

the base-line electrochemical data, and predict the influence of Fe enrichment on the rate of the HER. For the electrochemical tests, the working electrode area used was 1 cm^2; a saturated calomel electrode (SCE), and a Ti mesh counter electrode were also used to complete the three-electrode set-up. An electrochemical flat cell (Princeton Applied Research) was used in all the electrochemical tests, with the testing being done by a Bio-Logic VMP 3Z potentiostat. The tests were run using the EC-lab software. After cathodic polarization the samples were imaged using an optical microscope. It is assumed herein, that the surface Fe concentration of the three "standard" samples, are equal to bulk concentration and that the pre-polarized samples behave like Mg samples with different Fe content.

A Simple Model to Estimate Fe Enrichment during Anodic Polarization

It is assumed that the Mg surface, exposed to the electrolyte (in the three-electrode set-up) is a unit cylinder with the electrolyte-facing surface area 1 cm^2 and height of 5.2 Å (corresponding to the "c" lattice constant of the Mg hexagonal close packed unit cell).[26] Since the volume of this unit cylinder is thus known, and the density of Mg is 1740 kg/m^3,[26] one can calculate the mass of the Mg unit cylinder, and hence the number of Mg atoms in this unit cylinder (from Avogadro's laws). The number of Mg atoms in a Mg unit cylinder (with the above defined dimensions) is given as n_{Mg}. From Faraday's laws, on anodically polarising a Mg sample at a fixed current density, it is known that;

$$Q = It = x_{Mg_{diss}}.z.F \quad [1]$$

where Q is the applied charge (in coulomb), I is the applied current density in A/cm^2, t is time in seconds, $x_{Mg_{diss}}$ is number of moles of dissolved Mg, z is 2, and F is the Faraday constant (96485 coulomb/mole). The number of dissolved Mg atoms ($n_{Mg_{diss}}$) is calculated from $x_{Mg_{diss}}$ using Avogadro's laws. The number of unit cylinders of Mg dissolved is thus given by N_{diss}

$$N_{diss} = \frac{n_{Mg_{diss}}}{n_{Mg}} \quad [2]$$

It is assumed that all the Fe atoms remain and hence agglomerate/enrich on the Mg surface; the Fe concentration after dissolution of N_{diss} unit cylinders, present on the Mg surface (including those in the $N_{diss} + 1^{th}$ unit cylinder) is thus given by

$$[Fe_{theor.}] = (N_{diss} + 1).initial\,[Fe] \quad [3]$$

Since the variables in the given set of equations from (1–3), are the applied current (I) and polarization time (t), the final equation for$[Fe_{theor.}]$ can be simplified to:

$$[Fe_{theor.}] = ([1392.(I.t)] + 1).initial\,[Fe] \quad [4]$$

From Equation 4 the Fe enrichment in ppm, can be deduced from the initial Fe concentration and the applied anodic charge (given by *I.t*). This simple model assumes that all the Fe atoms upon the Mg surface are not dissolved during surrounding Mg dissolution and Equation 4 has been used to compute the Fe enrichment under different conditions of applied current, initial Fe concentration (in ppm) and time. This has been presented in the following section.

Results and Discussion

Cathodic polarization of Mg with different Fe concentration.— The cathodic polarization curves of Mg with three different Fe concentrations (40 ppm, 220 ppm and 13,000 ppm) are shown in Figure 1. As expected, the kinetics of the cathodic reaction (HER) increase with increasing Fe content. The cathodic currents (i_c) at −1.9 V_{SCE} (which is sufficiently below the Mg OCP) of the three different samples are shown in Figure 2. The i_c corresponding to pure Fe is also included in Figure 2 (taken from[27]). From this plot it can be inferred that with increase in the Fe content the HER current increases, and that the overall range for the HER current on Mg (with increasing Fe concentration) is from about 0.0003 to 0.008 A/cm^2. The Fe concentration [Fe] is

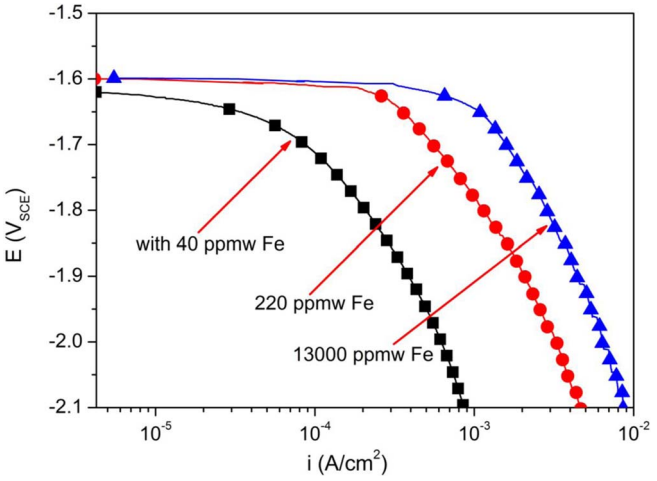

Figure 1. Cathodic polarization curves for Mg samples with three different concentrations of Fe: 40 ppm Fe, 220 ppm Fe and 13000 ppm Fe. The electrolyte used was 0.1 M NaCl, and the scan rate was 1 mV/s.

plotted on a logarithmic scale, and the relation between the cathodic current at −1.9 V_{SCE} and the Fe concentration in ppm (logarithmic) is nearly linear. This plot gives a quantitative estimation of the increase in the rate of HER with the increase in [Fe].

Theoretical Fe enrichment during anodic polarization.— The schematic of impurity enrichment during anodic polarization on the Mg surface is shown in Figure 3a–3d. Initially, the surface concentration of the impurities (such as Fe) is a few ppm. Once anodic polarization has commenced, the film on the pristine Mg surface undergoes "break-down", and Mg dissolves away with a few Fe atoms adhering to the surface (Figure 3a). The noble impurities such as Fe do not dissolve away from the Mg matrix, and they can only be mechanically dislodged. Assuming that mechanical dislodgement is zero, i.e. Fe enrichment is 100% efficient and all the Fe atoms agglomerate on the Mg surface, the Fe atoms will enrich the Mg surface, and also the bi-layered film formed on the Mg surface (Figure 3b–3c). The final anodically polarized surface will comprise Fe atoms or particles agglomerated on the Mg surface, or beneath or within the bi-layered film (Figure 3d). This bi-layered film is thick and dense, and may contain a large concentration of Fe atoms (Figure 3d). The model (given by Eqs. 1–3), assumes 100% Fe enrichment, with no Fe atoms mechanically removed from the Mg matrix, and Equation 4 is used to predict the theoretical Fe concentration [$Fe_{theor.}$] (in ppm), as a result of enrichment during anodic polarization. The [$Fe_{theor.}$] values for the

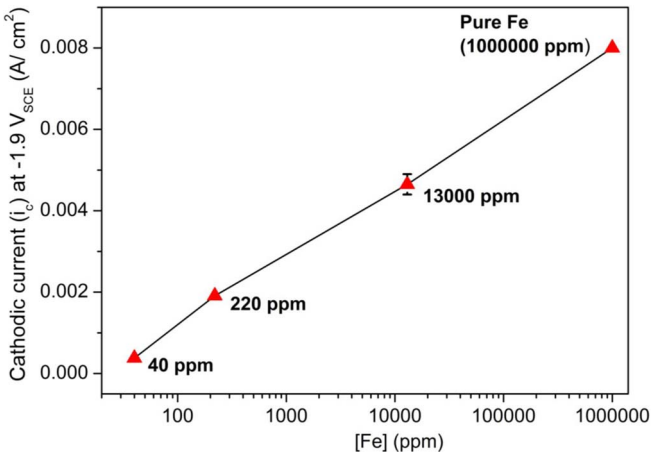

Figure 2. The cathodic current (i_c) recorded at −1.9 V_{SCE} for the Mg samples, as a function of the different Fe concentrations (40 ppm, 220 ppm and 13000 ppm Fe). The i_c for pure Fe (1000000 ppm) has also been included in this plot.

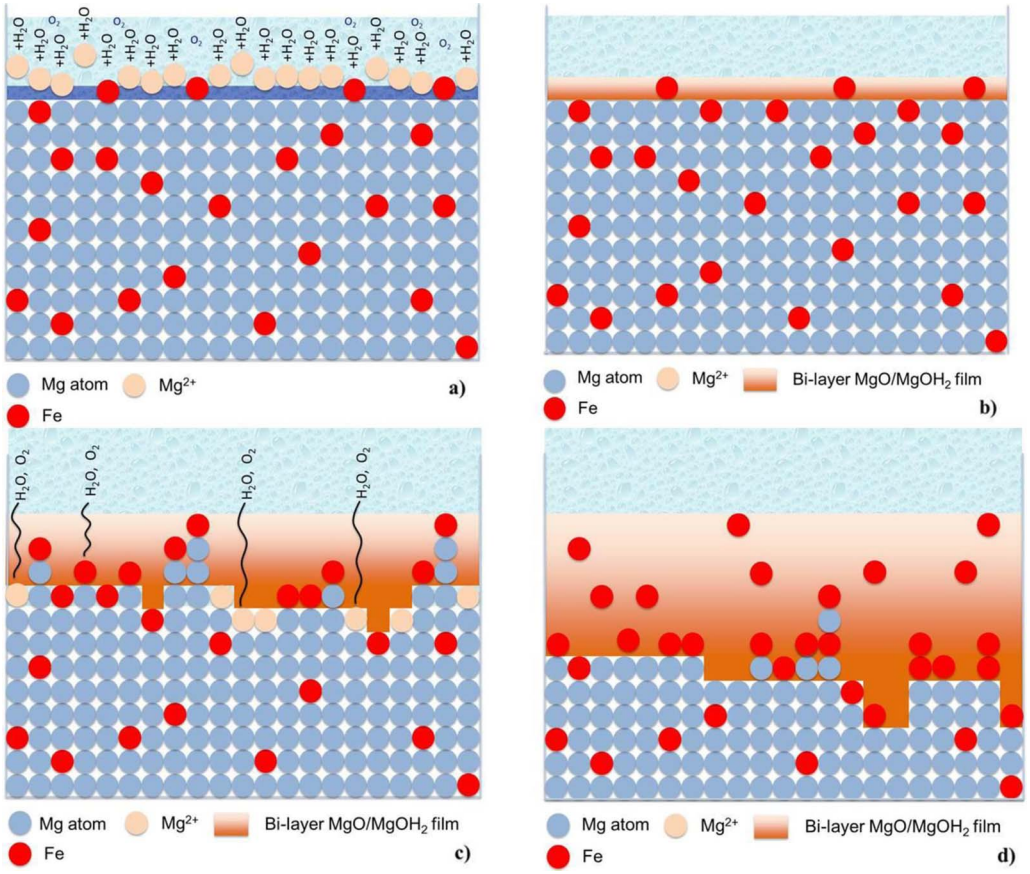

Figure 3. Phenomenological representations of Mg dissolution with noble metal impurities as a function of dissolution. a) As the film on the Mg surface undergoes breakdown, Mg dissolves as Mg^{2+} and some Fe atoms accumulate on the surface. b) With continued Mg dissolution, Fe atoms (or agglomerates) become present at the Mg surface and c) the evolution of a bi-layered film $MgO/Mg(OH)_2$ film occurs between the metal and the electrolyte. d) The dissolved Mg surface may comprise of Fe atoms or particles agglomerated on the Mg surface and beneath or in the bilayered film. It is assumed at all the Fe atoms having an electrical contact with the Mg surface serve as consistent cathodes.

different Mg systems, when anodically polarized at different current densities are shown in Figure 4. It is seen that Fe enrichment of the surface is rapidly attained at relatively short time scales (seconds to minutes) when the applied current densities are > 1 mA/cm^2. It must be noted that, in reality, Fe enrichment may not be 100% efficient as portrayed by Eq. 4, and rather, a large portion of Fe atoms/particles may be mechanically detached from the Mg matrix. In that case, they may not be micro-galvanically coupled to the Mg matrix, and thus may not serve as sites for the cathode reaction. It is assumed that all the Fe atoms having an electrical contact with the Mg surface serve as consistent cathodes. The relationship between [$Fe_{theor.}$] and the applied charge (*I.t*) is linear (which is not readily revealed in the semi-logarithmic plot presented in Figure 4).

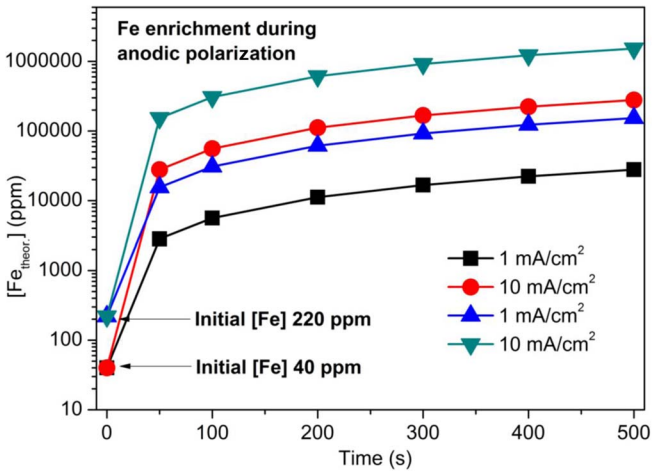

Figure 4. Theoretical Fe concentration ([$Fe_{theor.}$]) attained by Fe enrichment upon the Mg surface during anodic polarization, as estimated by the Equation 4. In this figure, [$Fe_{theor.}$] has been calculated for two different initial [Fe] values and two different applied current densities, as a function of time (using Equation 4).

Cathodic polarization of pre-anodically polarized Mg-Fe samples.— The 40 ppm Fe sample was anodically polarized at 1 mA/cm^2 for 50 seconds and 500 seconds, and also at 10 mA/cm^2 for 500 seconds. The resultant surfaces were all then subject to cathodic polarization to compare with the base-line (un-pre-polarized) electrochemical data, corresponding to the 40 ppm Fe sample (Figure 5a). For the sample pre-polarized for 50 s, the cathodic current at -1.9 V_{SCE} is almost equal to the cathodic current recorded for the base-line sample. However for samples pre-polarized for 500 s (with applied current density 1 mA/cm^2) there is a significant increase in the cathodic current at -1.9 V_{SCE}. For the sample pre-polarized at 10 mA/cm^2 for 500 s, the HER kinetics are much higher, and the cathodic current at -1.9 V_{SCE} is almost an order of magnitude higher than that of the base-line sample.

The 220 ppm Fe sample was anodically polarized for 200 seconds at 1 mA/cm^2 and at 10 mA/cm^2, and the resultant samples were subject to cathodic polarization, to compare with the base-line 220 ppm Fe sample (Figure 5b). Overall, the increase in the cathodic currents for this set of samples is not as high as seen for the 40 ppm Fe sample. For the Mg sample (with 220 ppm Fe) pre-polarized at 1

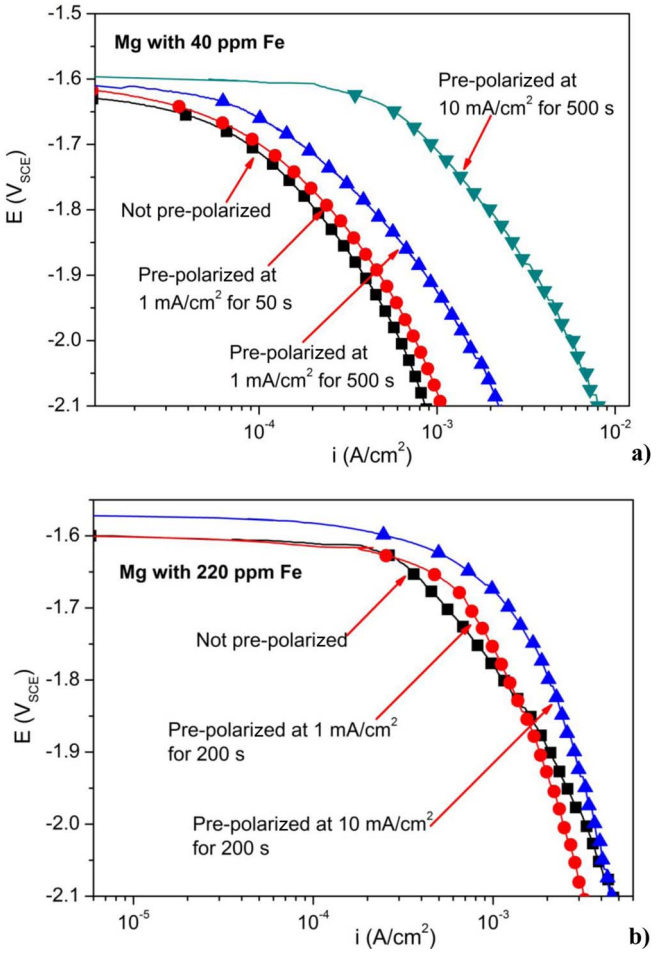

Figure 5. **a)** Cathodic polarization curves for Mg samples with 40 ppm Fe that were anodically pre-polarized for different time periods, and current densities. The base-line cathodic polarization curve for the 40 ppm Fe specimen (with no pre-polarization) has also been included. **b)** Cathodic polarization curves for Mg samples with 220 ppm Fe that were anodically pre-polarized for different time periods, and current densities. The base-line cathodic polarization curve for the 220 ppm Fe specimen (with no pre-polarization) is also shown.

mA/cm^2 (for 200 seconds), the HER current (at −1.9 V_{SCE}) is almost similar to that of the corresponding base-line sample, whereas, for the sample polarized at 10 mA/cm^2 the cathodic current is almost twice that of the base-line sample. The optical images of the above mentioned samples are shown in Figure 6. Additionally, the image of a 40 ppm Fe sample pre-polarized at 10 mA/cm^2 for 730 seconds is also displayed. It can be seen that with an increased coverage of dark regions, the rate of the HER increases upon the Mg surface, as reported by several researchers.[11,18–20] The surface coverage by the bi-layered film (dark region) increases with the applied anodic charge. It cannot be readily clarified on whether the growth rate of the film is completely influenced by the Fe concentration in the Mg matrix, as both the 40 ppm and 220 ppm samples are densely covered by the dark regions after prolonged anodic polarization (see Figure 6).

Fe enrichment and enhanced hydrogen evolution.— For the anodically polarized samples, [$Fe_{theor.}$] (arising from Fe enrichment after anodic polarization) was computed from Equation 4. Thus, for the 40 ppm Fe sample, anodically polarized at 1 mA/cm^2 for 50 s, the [$Fe_{theor.}$] calculated was around 2800 ppm. For the pre-polarization of 1 mA/cm^2 for 500 s, the [$Fe_{theor.}$] was calculated to be around 28,000 ppm, and for the 10 mA/cm^2 for 500 s sample the [$Fe_{theor.}$] was estimated as 278,440 ppm. Similarly, for the 220 ppm Fe sample, when the anodic polarization was 1 mA/cm^2 for 200 s, the [$Fe_{theor.}$] was calculated by Equation 4 to be around 61,000 ppm. For the sample pre-polarized at 10 mA/cm^2 for 200 s, the [$Fe_{theor.}$] corresponding to the enrichment, was calculated to be around 612,000 ppm.

The i_c values (taken from Figure 5a–5b) at −1.9 V_{SCE} for the different pre-polarized samples, are plotted against the corresponding [$Fe_{theor.}$] in Figure 7. These data are compared with a similar plot for actual [Fe] versus i_c (taken from Figure 2). $i_{c,a}$ is the actual cathodic current measured for the sample after being subject to anodic polarization, and $i_{c,t}$ corresponds to the cathodic current expected (according to the actual [Fe] vs i_c curve) if the Fe concentration on the Mg surface is [$Fe_{theor.}$]). $i_{c,t}$ thus corresponds to a cathodic current assuming that the Fe enrichment is a 100% efficient process (given by Equation 4), i. e. all the Fe particles/atoms enrich the Mg surface, and also serve as consistent cathodes. The point (i) represents the cathodic current (i_c) corresponding to the un-polarized sample (40 ppm sample) therefore represents the point (Initial [Fe], i_c). Initial [Fe] is the original Fe concentration (40 or 220 ppm). Point (ii) represents ([$Fe_{theor.}$], $i_{c,a}$) which corresponds to the actual cathodic current measured for an anodically polarized sample (40 ppm sample polarized at the current 10 mA/cm^2 for 500 s), and estimated by 4 to have a Fe concentration [$Fe_{theor.}$]. The expected cathodic current for an Mg sample having a Fe concentration [$Fe_{theor.}$] is given by point (iii) which is ([$Fe_{theor.}$], $i_{c,t}$). The values of $i_{c,a}$ and $i_{c,t}$ are similarly deduced for all the other anodically polarized samples.

The ratio of increase in the cathodic activity of Mg as a function of the applied anodic charge was calculated using 5, and is plotted as

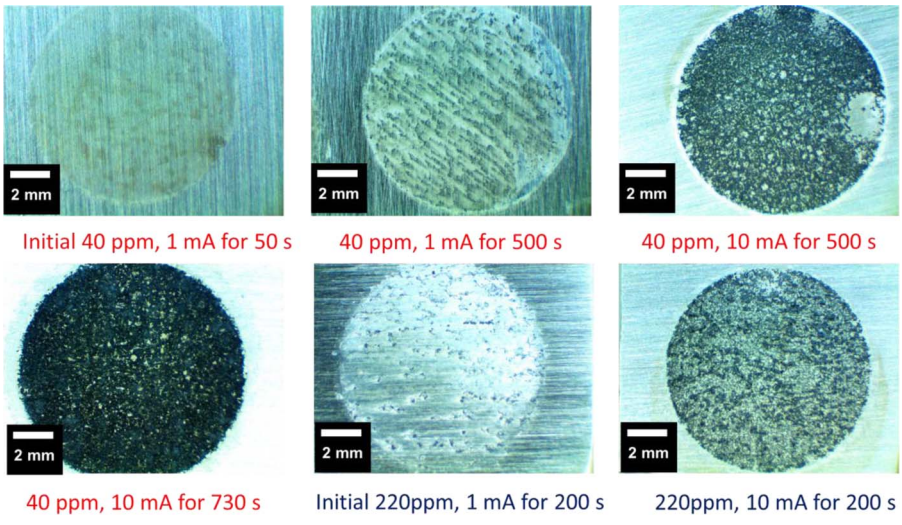

Figure 6. Optical images of specimen surfaces corresponding to the Mg samples with 40 ppm Fe and 220 ppm Fe, which were subject to anodic polarization at different conditions (as indicated in the images).

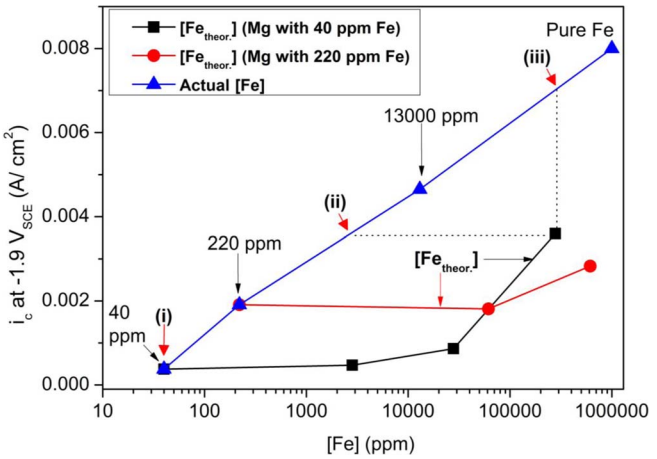

Figure 7. i_c at -1.9 V_{SCE} plotted as a function of [Fe]. Actual [Fe] corresponds to the data shown in Figure 2. [$Fe_{theor.}$] was deduced from the Equation 4 for the different anodic pre-polarization conditions of Mg samples. The i_c values corresponding to the different pre-polarization conditions were taken from Figure 5. (i) represents the point (Initial [Fe], i_c), (ii) represents the point (Actual [Fe], $i_{c,a}$) and (iii) represents the point ([$Fe_{theor.}$], $i_{c,t}$).

a function of the applied anodic charge in Figure 8. The actual [Fe] corresponding to Fe enrichment is also indicated at the different states of the applied charge in Figure 8.

$$Increase\ in\ cathodic\ activity = \frac{i_{c,a}}{i_c} \quad [5]$$

The model (given by Eqs. 1 to 3) assumed that all the Fe atoms remain attached to the Mg surface during and after anodic polarization, however, as seen by the difference between $i_{c,t}$ and $i_{c,a}$ in Figure 7, this process is not 100% efficient and most of the Fe atoms are likely dislodged from the Mg surface during anodic polarization. Therefore, for the anodically polarized samples $i_{c,a}$ was significantly lower than $i_{c,t}$. The cathodic enrichment efficiency was calculated by 6 using these values, and then plotted as function of applied charge accumulated during galvanostatic "pre-treatment" (Figure 9).

$$Cathodic\ Enrichment\ Efficiency = \frac{i_{c,a} - i_c}{i_{c,t} - i_c} \quad [6]$$

The Fe enrichment efficiency defined as the percentage of Fe atoms retained on the Mg surface during/after anodic polarization was computed using 7. This value was also plotted as a function of applied charge in Figure 10. This equation for Fe enrichment efficiency is valid only for anodically polarized samples, as for unpolarized samples, [$Fe_{theor.}$] is equal to Initial [Fe] in 7. The Fe enrichment efficiency for such an unpolarized sample is arbitrarily taken to be zero.

$$Fe\ Enrichment\ Efficiency = \frac{Actual\,[Fe] - Initial\,[Fe]}{[Fe_{theor.}] - Initial\,[Fe]} \quad [7]$$

For the Mg sample with 40 ppm Fe, the ratio of increase in cathodic activity is in the range 1–5 for applied anodic charge in the range 0.5 to 1 coulomb (Figure 8). However when a higher charge (around 5 coulomb) is applied the ratio of increase in cathodic activity is close to 10. For the 220 ppm Fe sample polarized at 1 mA/cm^2 for 200 s, the cathodic current is within the error-range of the unpolarized 220 ppm Fe sample (Figure 7), and therefore, the ratio of increase in cathodic activity is close to 1, and the cathodic enrichment efficiency and Fe enrichment efficiency are both zero.

It is worthwhile to note in Figure 7 that for the 220 ppm Fe sample polarized at 10 mA/cm^2 for 200 s the [$Fe_{theor.}$] is extremely high (at 612, 000 ppm). However, the cathodic current corresponding to this sample is much lower than that of the 40 ppm Fe sample polarized at 10 mA/cm^2 for 500 s (with [$Fe_{theor.}$] at 278,440 ppm. From Figure 6 it can be seen that the 40 ppm Fe sample (polarized at 10 mA/cm^2 for

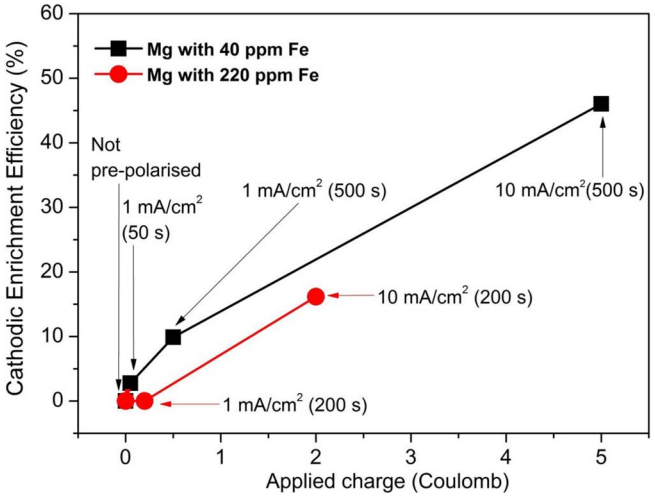

Figure 9. Cathodic enrichment efficiency (%) given by $[\frac{i_{c,a}-i_c}{i_{c,t}-i_c}]$ .100 plotted as a function of applied charge.

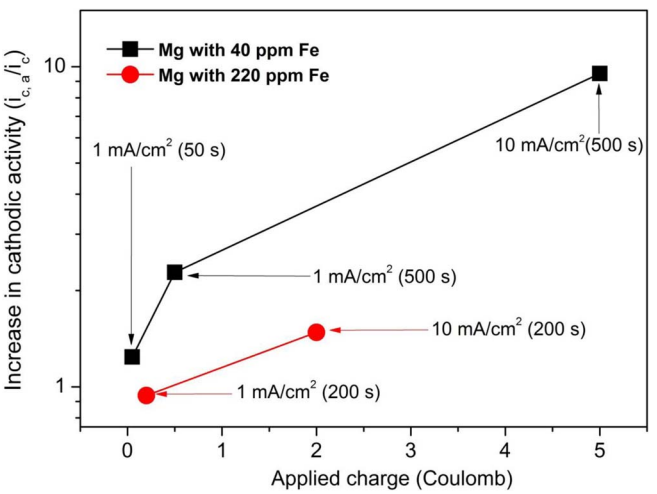

Figure 8. The ratio of increase in cathodic activity, on anodic polarization, plotted as a function of applied anodic charge.

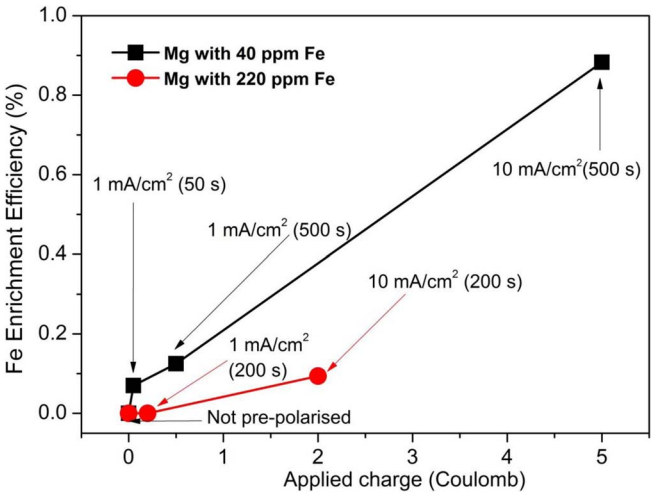

Figure 10. Fe enrichment efficiency (%) given by $[\frac{Actual[Fe]-Initial[Fe]}{[Fe_{theor.}]-Initial[Fe]}]$ .100 plotted as a function of applied charge.

500 s) is more densely covered by the dark film when compared to the 220 ppm Fe sample (polarized at 10 mA/cm^2 for 200 s). This set of observations suggest that the enhanced HER on anodically polarized Mg is not completely dictated by the Fe concentration in the Mg matrix, but there are other processes which enhance the HER upon anodically polarized Mg surfaces.

It can be seen in Figure 9 that for the Mg sample with 40 ppm Fe, the cathodic enrichment efficiency increases steadily with the applied anodic charge, and reaches close to 50% for the sample anodically polarized at 10 mA/cm^2 for 500 s (5 coulomb). For the 220 ppm Fe sample the cathodic enrichment efficiency is close to 20% for the sample with the applied anodic charge of 2 coulomb. The Fe enrichment efficiencies at moderate applied anodic charges (below 1 coulomb) for both the 40 ppm and 220 ppm Fe samples are low and in the range 0 to 0.2% (Figure 10). However, for high quantities of applied charge passed (near 5 coulomb) the Fe enrichment efficiency tends toward 1%.

Overall it is observed that the cathodic current at -1.9 V_{SCE} (corresponding to the HER kinetics) increases linearly with logarithm of [Fe] (in ppm) regardless of the solubility limit of Fe in Mg, thus providing a quantitative basis to relate the Fe concentration in Mg, to phenomena such as the negative difference effect, and enhanced catalytic activity for the HER during anodic polarization.[25] The efficiency of Fe enrichment is poor and less than 1% of the Fe atoms/particles ideally expected to enrich the Mg surface during the anodic polarization of pure Mg actually serve as consistent cathodes in the system. Since the HER kinetics varies linearly with the logarithm of [Fe], the effect of surface Fe enrichment on HER kinetics during anodic polarization is more pronounced for Mg systems with low initial [Fe]. This work also suggests that [Fe] may not completely control the HER kinetics on the Mg surface during anodic polarization.

Validation

Cain et al.[28] performed Rutherford Backscattering Spectrometry (RBS) on anodically polarized Mg samples, to detect Fe enrichment upon the Mg surface, after anodic polarization. The atom fraction of Fe (in %) for an un-corroded, pristine Mg surface (99.9% pure), as determined using RBS, was found to be in the range 0.0003 to 0.0004%.[28] After anodic polarization at -1.625 V_{SCE} for 24 hours, RBS revealed that the Fe concentration on the Mg surface increased to be in the range 0.001 to 0.0028%.[28] Therefore, in this case, there is over an order of magnitude increase in the Fe concentration on the Mg surface during anodic polarization. However, the overall Fe concentration is still very low ($\ll$1%), implying that the Fe enrichment efficiency is very poor. The work by Cain et al.[28] thus validates some of the findings of the current work; on the Fe enrichment efficiency upon Mg during anodic polarization being poor (less than 1% efficient). In a separate body of work Fajardo et al[29] studied the effect of impurities on the kinetics of the HER on high purity Mg (99.98% Mg) and ultra-high purity Mg (99.9999% Mg), by measuring the H_2 gas evolved during anodic polarization. It was observed that the rate of HER during anodic polarization, was very high even for the ultra-high purity Mg samples,[29] implying that impurity enrichment (Fe enrichment) alone does not principally contribute to the enhanced HER upon Mg during anodic polarization.

Conclusions

Mg specimens with different concentrations of Fe (40, 220 and 13,000 ppm) were subject to cathodic polarization, and the cathodic current of each of these samples at -1.9 V_{SCE} were plotted as function of the logarithmic Fe concentration [Fe] (in ppm). The relation between actual [Fe] (logarithmic) and the cathodic current was found to be nearly linear and thus provides a quantitative estimate to predict the hydrogen evolution reaction (HER) rates on Mg based on their actual Fe concentration.

A phenomenological model for predicting Fe enrichment at the Mg surface during anodic polarization was presented, assuming that the Fe is not oxidized in the range of potentials at which Mg is oxidized, and that Fe enrichment is ideal (i.e. 100% efficient). The [Fe] corresponding to different states of anodic polarization (by varying the current density and time of polarization) were calculated by this model, and represented as [$Fe_{theor.}$]. The Mg specimens with 40 ppm and 220 ppm Fe were anodically polarized at different conditions, and then cathodically polarized to determine the cathodic current at -1.9 V_{SCE}. Based on the anodic polarization conditions, a [$Fe_{theor.}$] was determined and a plot of [$Fe_{theor.}$] vs cathodic current was made, and compared with the plot of actual [Fe] vs cathodic current. This plot was used to compute the increase in the cathodic activity of Mg (as a function of [Fe]), the cathodic enrichment efficiency, and hence, the Fe enrichment efficiency.

The Fe enrichment efficiency is poor, when the anodic polarization is moderate ($<$ 0.5 coulomb for the 40 ppm Fe sample and $<$ 2 coulomb for the 220 ppm Fe alloy) and the efficiency of enrichment is between 0 to 0.2%. This implies that most of the Fe atoms/particles are either dislodged from the Mg surface during anodic polarization (i.e. undermined), or entrapped in the oxides making them less-effective as cathodes, or that accumulation simply may not occur according to the phenomenological model presented. For high anodic polarization ($>$ 5 coulomb) the Fe enrichment efficiency tends toward 1% for the 40 ppm Fe sample.

The rate of the cathodic reaction upon Mg-Fe samples increases following anodic polarization, however, the rate of increase is more pronounced for Mg samples with low initial [Fe], since the HER rate is seen to vary with the logarithm of [Fe]. It can be implied from the work herein, that [Fe] may not principally completely control the HER kinetics on the Mg surface during anodic polarization. The accumulation of Fe is fractionally, not principally responsible for the documented enhanced catalytic response of Mg following Mg dissolution.

Acknowledgment

Authors D. Lysne and S. Thomas contributed equally to this work.

References

1. A. A. Nayeb-Hashemi, J. B. Clark, and L. J. Swartzendruber, The Fe-Mg (Iron-Magnesium) System, *Bulletin of Alloy Phase Diagrams*, **6**, 235 (1985).
2. T. Haitani, Y. Tamura, T. Motegi, N. Kono, and H. Tamehiro, Solubility of iron in pure magnesium and cast structure of Mg-Fe alloy, *Materials Science Forum*, **419–422**, 697 (2003).
3. D. S. Gandel, M. A. Easton, M. A. Gibson, and N. Birbilis, CALPHAD Simulation of the Mg(Mn,Zr)–Fe System and Experimental Comparison with As-cast Alloy Microstructures As Relevant to Impurity Driven Corrosion of Mg-alloys, *Materials Chemistry and Physics*, **143**, 1082 (2014).
4. S. Simanjuntak, M. K. Cavanaugh, D. S. Gandel, M. A. Easton, M. A. Gibson, and N. Birbilis, The influence of iron, manganese and zirconium on the corrosion of magnesium: An artificial neural network approach, *Corrosion*, **71**, 199 (2015).
5. S. Akavipat and E. B. Hale, Effects of iron implantation on the aqueous corrosion of magnesium, *Materials Science and Engineering*, **69**, 311 (1985).
6. J. E. Hillis, The effect of heavy metal contamination on magnesium corrosion performance, *Light Metal Age, SAE (Detroit)*, 25 (1983).
7. J. A. Boyer, The corrosion of magnesium and of the magnesium aluminum alloys containing manganese, *American Magnesium Corporation*, 417 (1927).
8. R. E. McNulty and J. D. Hanawalt, Some corrosion characteristics of high purity magnesium, in: R. B. Mears (editor), *Eighty-first general meeting, Transactions of the Electrochemical Society*, 423 (1942).
9. J. D. Hanawalt, C. E. Nelson, and J. A. Peloubet, Corrosion Studies of Magnesium and Its Alloys, *Trans AIME*, **147**, 273 (1942).
10. K. Gusieva, C. H. J. Davies, J. R. Scully, and N. Birbilis, Corrosion of Magnesium: the role of alloying, *International Material Reviews*, **60**, 169 (2015).
11. M. Taheri, J. R. Kish, N. Birbilis, M. Danaie, E. A. McNally, and J. R. McDermid, Towards a physical description for the origin of enhanced catalytic activity of corroding magnesium surfaces, *Electrochimica Acta*, **116**, 396 (2014).
12. D. S. Gandel, N. Birbilis, M. A. Easton, and M. A. Gibson, Iron and corrosion control in aluminium-free magnesium alloys, in: W. J. Poole and K. U. Kainer (editors) *Magnesium 2012, 9th International Conference on Magnesium Alloys and Applications*, 197 (2012).
13. D. S. Gandel, M. A. Easton, M. A. Gibson, and N. Birbilis, Influence of Mn and Zr on the Corrosion of Al-Free Mg Alloys: Part1 – Electrochemical Behavior of Mn and Zr, *Corrosion*, **69**, 666 (2013).
14. T. Cain, L. G. Bland, N. Birbilis, and J. R. Scully, A compilation of corrosion potentials for magnesium alloys, *Corrosion*, **70**, 1043 (2014).
15. N. T. Kirkland, J. Lespagnol, N. Birbilis, and M. P. Staiger, A survey of bio-corrosion rates of magnesium alloys, *Corrosion Science*, **52**, 287 (2010).

16. W. Beetz, On the Development of Hydrogen from the Anode, *Philosophical Magazine Series* **4**, 269 (1866).
17. R. Glicksman and R. Anodic Dissolution of Magnesium Alloys in Aqueous Salt Solutions, *Journal of the Electrochemical Society*, **106**, 83 (1959)
18. G. Williams, N. Birbilis, and H. N. McMurray, The Source of Hydrogen Evolved from a Magnesium Anode, *Electrochemistry Communications*, **36**, 1 (2013).
19. M. Curioni, The Behaviour of Magnesium During Free Corrosion and Potentiodynamic Polarization Investigated by Real-Time Hydrogen Measurement and Optical Imaging, *Electrochimica Acta*, **120**, 284 (2014).
20. N. Birbilis, A. D. King, S. Thomas, G. S. Frankel, and J. R. Scully, Evidence for Enhanced Catalytic Activity of Magnesium Arising from Anodic Dissolution, *Electrochimica Acta*, **132**, 277 (2014).
21. S. Lebouil, A. Duboin, F. Monti, P. Tabeling, P. Volovitch, and K. Ogle, A Novel Approach to On-Line Measurement of Gas Evolution Kinetics: Application to the Negative Difference Effect of Mg in Chloride Solution, *Electrochimica Acta*, **124**, 176 (2014).
22. L. Rossrucker, K. J. J. Mayrhofer, G. S. Frankel, and N. Birbilis, Investigating the Real Time Dissolution of Mg Using Online Analysis by ICP-MS, *Journal of the Electrochemical Society*, **161**, C115 (2014).
23. S. Lebouil, O. Gharbi, P. Volovitch, and K. Ogle, Mg Dissolution in Phosphate and Chloride Electrolytes: Insight Into the Mechanism of the Negative Difference Effect, *Corrosion*, **71**, 234 (2015).
24. G. S. Frankel, A. Samaniego, and N. Birbilis, Evolution of Hydrogen at Dissolving Magnesium Surfaces, *Corrosion Science*, **70**, 104 (2013).
25. S. Thomas, N. V. Medhekar, G. S. Frankel, and N. Birbilis, Corrosion Mechanism and Hydrogen Evolution on Mg, *Current Opinion in Solid State and Materials Science*, **19**, 85 (2015).
26. G. W. C. Kaye and T. H. Laby, *Tables of Physical and Chemical Constants*, Longman Scientific and Technical, 16th Edition (1995).
27. S. H. Salleh, S. Thomas, J. A. Yuwono, K. Venkatesan, and N. Birbilis, Enhanced hydrogen evolution on $Mg(OH)_2$ covered Mg surfaces, *Electrochimica Acta*, **161**, 144 (2015).
28. T. Cain, S. B. Madden, N. Birbilis, and J. R. Scully, Evidence of the Enrichment of Transition Metal Elements on corroding Magnesium surfaces using Rutherford Backscattering Spectrometry, *Journal of the Electrochemical Society*, **162**, C228 (2015).
29. S. Fajardo and G. S. Frankel, Effect of impurities on the enhanced catalytic activity for hydrogen evolution in high purity magnesium, *Electrochimica Acta*, **165**, 255 (2015).